



**HAL**  
open science

## Experimental study of the air–steam mixture leakage rate through damaged and partially saturated concrete

Sonagnon Medjigbodo, Marta Choinska, Jean-Pierre Regoin, Ahmed Loukili, Abdelhafid Khelidj

► **To cite this version:**

Sonagnon Medjigbodo, Marta Choinska, Jean-Pierre Regoin, Ahmed Loukili, Abdelhafid Khelidj. Experimental study of the air–steam mixture leakage rate through damaged and partially saturated concrete. *Materials and structures*, 2015, 49 (3), pp.843-855. 10.1617/s11527-015-0542-5. hal-04736516

**HAL Id: hal-04736516**

<https://hal.science/hal-04736516v1>

Submitted on 15 Oct 2024

**HAL** is a multi-disciplinary open access archive for the deposit and dissemination of scientific research documents, whether they are published or not. The documents may come from teaching and research institutions in France or abroad, or from public or private research centers.

L'archive ouverte pluridisciplinaire **HAL**, est destinée au dépôt et à la diffusion de documents scientifiques de niveau recherche, publiés ou non, émanant des établissements d'enseignement et de recherche français ou étrangers, des laboratoires publics ou privés.



Distributed under a Creative Commons Attribution - NonCommercial 4.0 International License

# Experimental study of the air–steam mixture leakage rate through damaged and partially saturated concrete

Sonagnon Medjigbodo · Marta Choinska ·  
Jean-Pierre Regoin · Ahmed Loukili ·  
Abdelhafid Khelidj

**Abstract** This study is focused on the tightness of containment walls of nuclear power plants in case of loss of coolant accident. This kind of accident results in the rise from ambient conditions to a temperature of 140 °C and an air–steam mixture pressure of 5.2 bars. This rise creates high hydric, thermal and mechanical stress in concrete, impairing the tightness integrity of concrete wall. In this work, we propose to highlight experimentally the influence of initial water content of the sample, the compressive load and the percolating fluid on the hydraulic behavior of concrete. The tests are carried out on hollow cylindrical samples, using a device which allows to generate a gas mixture at the inlet and to measure the leakage rate at the outlet of the samples. As the tests are performed in isothermal conditions, the results show that at stress levels lower than 70–80 % of the peak stress, the leakage rate of the mixture is slightly influenced by both parameters (degree of saturation and stress). However, it can be noted that as the load exceeds this threshold value, the

damage effect due to mechanical loading remains more important in the leakage rate evaluation.

**Keywords** Steam · Damage · Degree of saturation · Leakage · Condensation · Relative humidity

## 1 Introduction

Permeability of concrete is commonly used as a key index for assessing the durability of concrete, especially when concrete is exposed to aggressive environments. In the specific case of nuclear power plants, the concrete structure must be sufficiently confined and leak-tight both in service life and in the event of Loss Of Coolant Accident (LOCA). This kind of disaster proceeds with simultaneous effects of temperature (140 °C) and gas (a mix of air and steam) of pressure (5 bars) exerted on one face, with the other side remaining at atmospheric conditions [39]. In this case, the rate of gas escape must be below 1.5 % of the confined gas volume per day [4]. As this criterion is not practically measurable, the nuclear power plants safety is evaluated by measuring the air leak flow through the inner containment wall at ambient temperature. So, in order to improve the knowledge of the link between the two situations and the understanding of the transfer's phenomenon in case of LOCA, some experimental full-scale leakage tests were performed: either on concrete without reinforcement and “cracking” [4, 39] or on reinforced concrete

---

S. Medjigbodo · J. P. Regoin · A. Loukili (✉)  
LUNAM Université, Centrale Nantes, Institut de  
recherche en Génie Civil et Mécanique (GeM) UMR  
CNRS 6183, 1 rue de la Noe, BP 92101,  
44321 Nantes Cedex 3, France  
e mail: ahmed.loukili@ec nantes.fr

M. Choinska · A. Khelidj  
LUNAM Université, Université de Nantes, IUT de Saint  
Nazaire, Institut de recherche en Génie Civil et  
Mécanique (GeM) UMR CNRS 6183, 58 rue Michel  
Ange, BP 420, 44600 Saint Nazaire, France

walls subjected to tensile load [17, 20]. In each case, an experimental setup was developed. It consists of a mechanical set-up [17, 20] which determines cracks through the wall and a thermo-hydraulic set-up [4, 17, 20, 39] which allows producing an air steam mixture in order to reproduce accidental scenarios. These studies show that during the heating of concrete, several non-linear and coupled mechanisms are involved [15]. The main phenomena that can be observed are heat conduction, water vapor diffusion, water flow due to pressure gradients and capillary effects, latent heat transfer due to water phase change (hydration dehydration process, adsorption desorption phenomena...) inside the pores... [12, 15]. It results in the significant changes to the material's inner structure and properties such as the increase in porosity and the degradation of strength properties. On the other hand, the air + steam percolation induces major mechanisms such as: steam condensation inducing plugging of concrete cracks and porosity, closing of cracks due to thermal induced compression... [17]. Because of the complexity of phenomena involved, coupled thermo-hydro-mechanical (THM) models are proposed in literature to assess the thermo-hydraulic and the mechanical behavior of concrete structures [9, 12, 13, 27] under LOCA or at high temperature. Some of these models have been validated against results of available experiments showing their usefulness in understanding and predicting concrete performance [9, 32, 40].

However, considering the evolution of the leakage rate through the porous media, it is closely related to the changes in permeability during the LOCA loading. Physical, chemical and mechanical processes that result from the ageing process and LOCA scenarios also generate cracks in the concrete structure. Accordingly, it is significant to understand the effects and the interaction of some parameters (damage, temperature and initial degree of saturation) on the air and air steam mixture flow properties of concrete.

Many research studies have been performed to investigate the permeability of concrete subjected to thermal stresses [6, 11, 23, 24, 34, 44] and mechanical loadings [6, 21, 29, 36, 41]. It was reported that the intrinsic permeability evolves exponentially with diffuse damage ( $D < 0.25$ ) [36]. Sugiyama et al. [41] and Choinska et al. [6] showed two important phases in the evolution of the permeability of concrete under compressive loading. The first phase consists in the slight decrease of the permeability and the second which

occurs after 80 % of the ultimate strength, where the permeability increases significantly. Gallé and Sercombe [11], Zeiml et al. [44] ... observed a significant increase in permeability for large temperatures (above 105 °C). According to the authors, this increase is due to several phenomena such as removal of free water from the capillary porosity, dehydration process (above 120 °C according to Noumowé et al. [34] and probably thermal deformation. Other studies show that the overall evolution of the permeability  $k$  due to damage and temperature follows a multiplicative format:  $k = f(\text{damage}) g(\text{temperature})$  [6, 14]. It means that the increase of intrinsic permeability of concrete subjected to thermo-mechanical loading is the products of two functions ( $f$  and  $g$ ) which reflect the contribution of each parameter separately. It is important to note that the above relationship were experimentally proved by [6] for a moderate compressive damage generated on ordinary concrete and by [14] for high-performance concrete (HPC) where damage is not only thermal but also mechanical. Moreover, in Gawin et al. [14], gas pressure plays an important role and should be also taken into account. Concerning cracked concrete (localized or single residual cracks), a sharp increase of gas flow and permeability has been observed [37, 42, Greiner et al. 18]. All of these results assume that the concrete is dry. When the concrete is partially saturated, Jacobs [22], Abbas et al. [1], Picandet et al. [36], Villain et al. [43], Monlouis-Bonnaire et al. [31], Kameche et al. [26] observed that permeability is not intrinsic. It was found that permeability decreases with increase of degree of saturation. The coupled effect of concrete moisture content and the compressive stresses on its permeability has also been studied [28, 36, 41]. It showed that when the concrete is damaged, only the crack pattern controls the overall gas flow and the increase of permeability is independent of the sample's moisture content. However, the presence of water in concrete significantly affects its permeability when the compressive stress level is less than 70 80 % of ultimate strength.

In these important studies, permeability to dry gas (oxygen, nitrogen) is preferred compared to permeability to water or water vapor. The main reason is that with water or water vapor, several complex and interrelated physical phenomena (rehydration, condensation, ...) would occur. Due to the difficulty and the lack of available and appropriate methods for the measurement of the air steam mixture transfer through concrete at high

temperature, a limited number of studies have been done on concrete material [19]. Moreover, these studies did not take into account all the parameters influencing the behavior of concrete material in LOCA conditions. Thus, more understanding is needed.

In our previous study, the coupled effects of compressive mechanical loading and free water content on dry gas (nitrogen) permeability of concrete [28] have been shown. The measurement of the air and steam mixture leakage rate through *dry concrete* samples under conditions ( $T = 140^\circ \text{C}$ ,  $P = 5$  bars and  $\text{RH} = 75\%$ ) close to LOCA conditions has also been performed [28]. However, using dry concrete is not justified because it is not realistic. Although the saturation state of concrete structures is not well known, it is obvious that in situ, the concrete is never completely dry. So, to be realistic, we need to take into account the influence of the degree of saturation in the analysis and prediction of air and water vapor leakage rates through partially damaged concrete. The aim of the work reported here is to determine the effect of degree of saturation and the coupled effect of degree of saturation – compressive stress level on the evolution of the gas mixture (nitrogen + steam) leakage rate.

## 2 Experimental program

### 2.1 Materials, curing and conditioning

The experiments were carried out on an ordinary concrete with a water/cement (W/C) ratio of 0.57. The cement used was CEM II/A-LL 42.5R and the maximum diameter of gravels was 25 mm. The mixture proportion is given in Table 1. Hollow cylindrical samples (110 mm in external diameter, 14 mm in internal diameter and 220 mm high) were cast following the European standards (EN 206-1). The average strength and porosity are reported as 40 MPa and 14 %. The average standard deviation is equal to 0.77 MPa and 0.8 % for the compressive

strength and the porosity respectively. More details about the materials, casting and curing procedure can be found in our previous research [28].

To study the influence of the water content of concrete on the gas permeability measurement, four water saturation levels  $S_r$  have been selected. For each water saturation level, two samples were tested. The moisture conditioning of the samples was obtained as described in Fig. 1 and detailed in Medjigbodo et al. [28]. It can be summarized as follows:

- (1) Long lime-saturated water curing after which concretes are assumed to be fully water-saturated.
- (2) Complete oven-drying at  $80^\circ \text{C}$ .
- (3) Partial water saturation process.

Figure 2a and b show respectively the time evolution of the sample's weight and their weight loss or gain during conditioning phase. It can be observed that, at  $80^\circ \text{C}$ , the removal of free moisture from the samples is reached rather quickly during the early stages of exposure. About 80-95 % of the free moisture in concrete is driven out after 2 weeks. Unlike concrete drying [3] or wetting (Fig. 2a, b) at  $20^\circ \text{C}$ , where slower drying/wetting kinetics takes place, the drying kinetics are quite fast at  $80^\circ \text{C}$ . Moreover, as illustrated in Fig. 2a, b, the absorbed water increases quickly for a period of a few days. It should also be noted that after the water immersion phase (or during the drying process), the distribution of water through the material is not homogeneous and a moisture gradient should appear [38]. Despite the conditioning method used, a homogeneous redistribution of the water in the samples cannot be expected before several years. So the tests were performed with a non-homogeneous distribution of moisture and the average saturation level was considered representative of the condition of the material.

The average mechanical response of concrete in uni-axial compression is illustrated in Fig. 3: after the storage in water (at 28 days) and after drying at  $80^\circ \text{C}$ .

**Table 1** Concrete constituents and mix proportions

Ingredient	Cement	River sand (0/5)	Gravel (5/12.5)	Gravel (12.5/25)	Effective water	Plasticizer
kg/m <sup>3</sup>	350	772	316	784	201	1.23
W/C ratio = 0.57						
Slump = 9 cm						

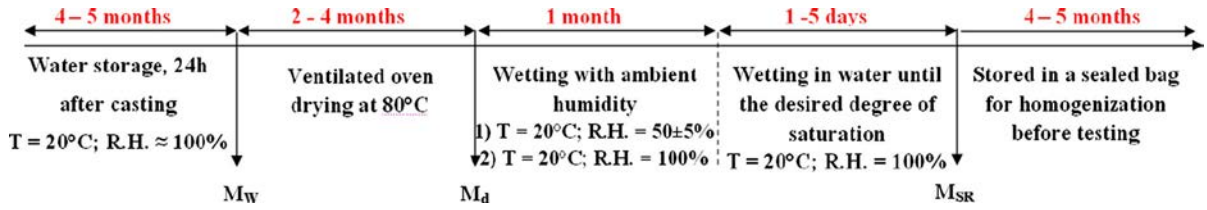


Fig. 1 Samples curing and conditioning processes

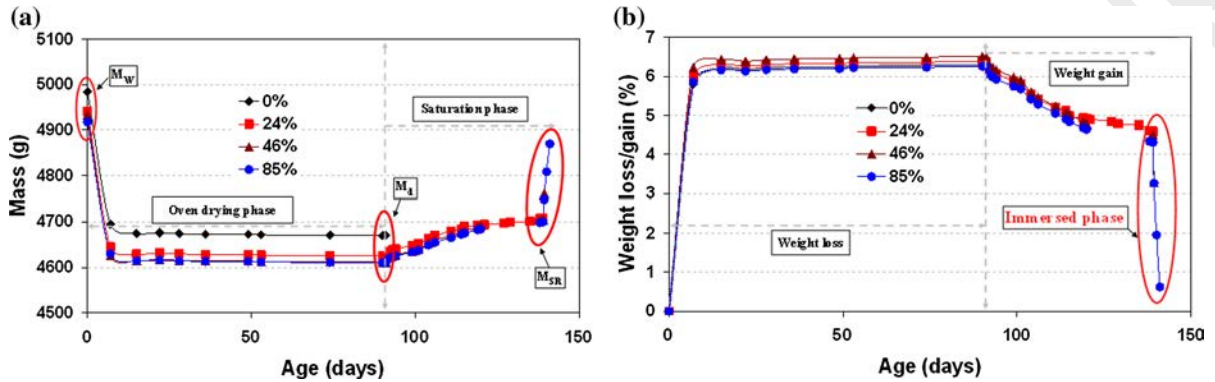


Fig. 2 a Weight versus duration. b Weight loss or gain versus drying or wetting time graphs of concrete samples

It can be seen in Fig. 3 that the change in moisture content caused by drying has a considerable effect on the mechanical properties of concrete. The compressive test results indicate that there was a partial gain in strength after drying process. The magnitude of strength gain is about 10 %.

## 2.2 Experimental set-up and test procedure

The experimental set-up illustrated in Fig. 4 was used to perform the permeability tests. A complete description

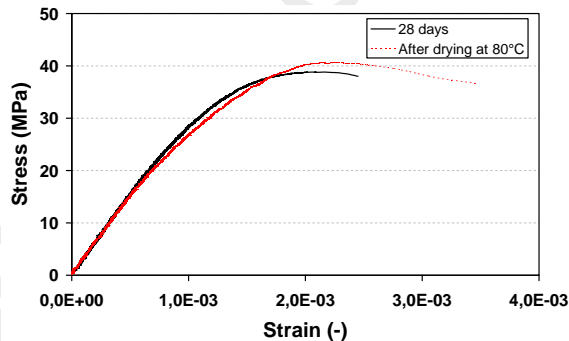


Fig. 3 Stress axial strain curves of the concrete (test performed at ambient temperature, mean curves)

of this test is given in Medjigbodo et al. [28]. It consists in:

firstly, imposing a uniform temperature to all parts of the device (test tube, cylinder, temperature and humidity sensors) placed inside the climatic chamber (Fig. 4) in order to avoid any steam condensation in the experimental device, secondly, injecting the air (nitrogen) steam mixture into the cylindrical borehole under the conditions close to LOCA scenario (Table 2).

The flow is radial. The relative pressure (difference between the injection pressure and the atmospheric pressure) is maintained until gas flow stabilization where the relative humidity (RH) of the output gas mixture and the air (nitrogen) flow rate are measured.

The full testing procedure is summarized as follows:

- First, the required temperature is applied (140 °C) at a constant rate of 10 °C/h during 24 h.
- After the heating phase, the nitrogen is injected at 5 bars until gas flow stabilization. The mass flow rate is measured at the downstream of the sample by the thermal mass flow meter (MFM)

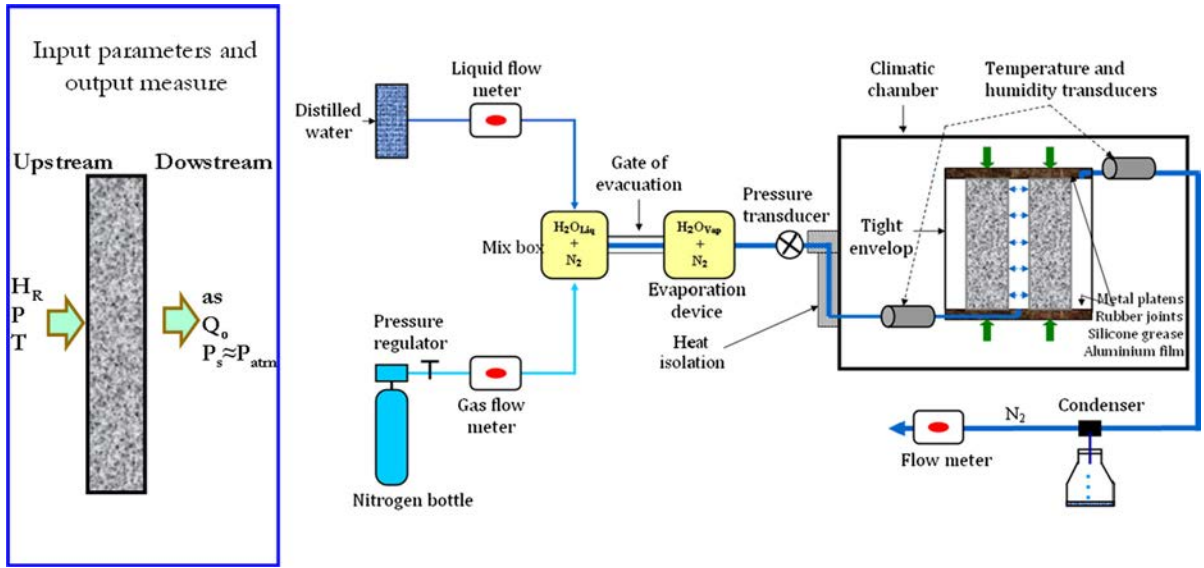


Fig. 4 Schematic illustration of test equipment [28]

Table 2 Parameters imposed at sample input and output

Input			Output
Temperature (°C)	Absolute pressure (bars)	Relative humidity (%)	Pressure (bar)
140	5	75	1

which converts the mass flow rate to an equivalent volumetric gas flow.

- (c) The gas mixture is then injected in experimental conditions given in Table 2.
- (d) At mix flow stabilization, a compressive loading is applied on the sample up to the required load level (Fig. 5). Load levels correspond to 20, 40, 60, 80, 90 and 95 % of the estimated peak stress in the pre-peak regime.

### 3 Results and discussion

All of the tests are performed as described in Sect. 2.2. It is important to note that a uniform temperature superior to dew point temperature is needed in order to avoid any thermal condensation. So, during the test, the temperature of 140 °C is kept in climatic chamber.

Two parameters are used to characterize the gas mixture flow through concrete: the output absolute humidity ( $a_s$ ), i.e. the amount of water vapor in a unit

volume of humid gas mixture extracted at the outlet of the sample, and the nitrogen flow rate ( $Q_0$ ).  $a_s$  is calculated from the value of the RH of the output gas mixture [28].

#### 3.1 Characterization of gas mixture flow through dry and undamaged concrete

In our previous study, the evolution of both parameters ( $a_s$  and  $Q_0$ ) were highlighted for dry and undamaged concrete samples submitted to experimental conditions, such as  $T = 120$  °C,  $P_t = 3.4$  bars and  $RH = 80$  % [28]. In order to investigate the effect of boundary conditions on the leakage rate value, the same tests are carried out with the experimental conditions given in Table 2. The results presented in Fig. 6 clearly show the same phase evolution as those obtained in Medjigbodo et al. [28]: a capillary condensation phase (phase 1), a transient phase (phase 2) and a stabilization phase (phase 3). It is important to note that the evolution of both parameters seems to be

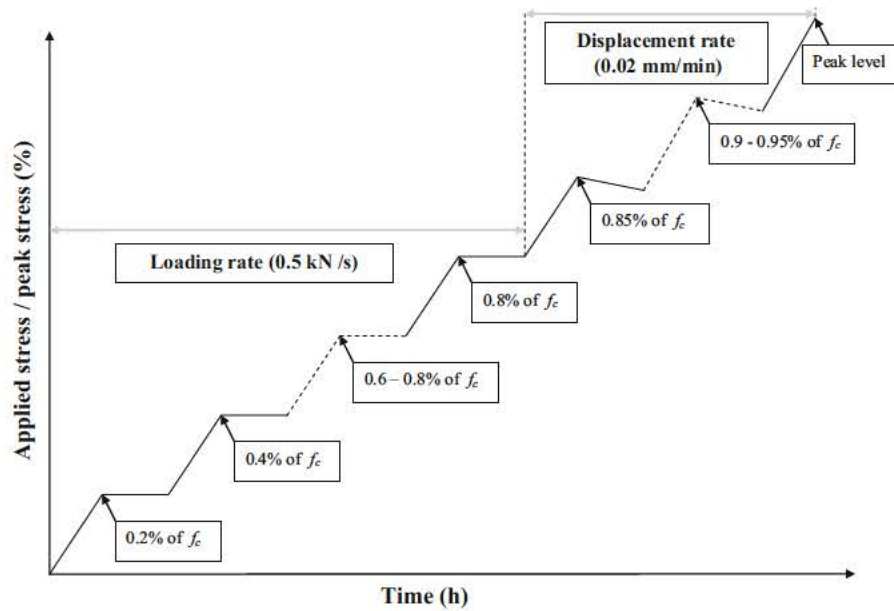


Fig. 5 Loading program

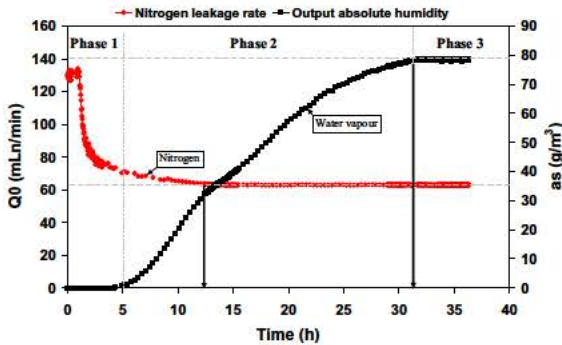


Fig. 6 Evolution of the output absolute humidity and the leakage rate of dry air through dry concrete sample

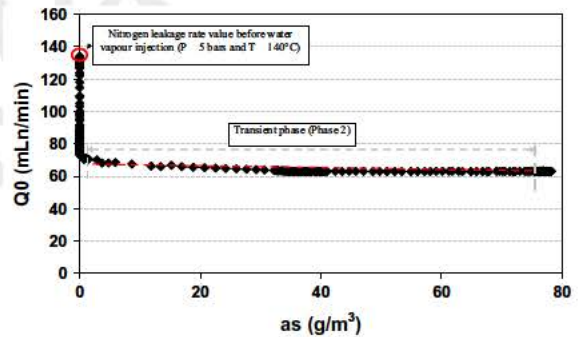
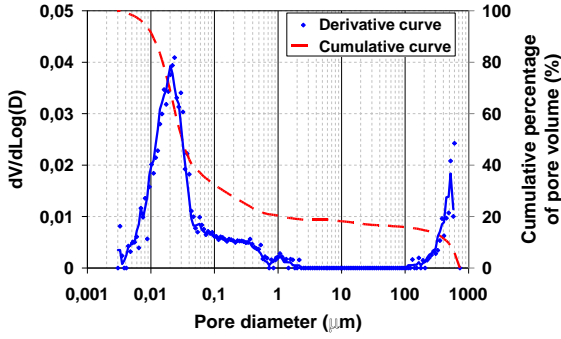


Fig. 7 Leakage rate of dry air versus output absolute humidity graph of dry concrete sample

linear in the transient phase (phase 2) (Fig. 7). When the output absolute humidity increases, the nitrogen flow rate decreases. Moreover, it should be noted that if the device (Fig. 4) allows recovering a steam at the downstream of the sample, it is unknown in what phase it goes out. However, it could be assumed that if the porosity of the concrete is sufficiently small, the condensation phenomenon may cause a significantly continuous capillary phase and liquid flow should occur [7, 8]. Moreover, the downstream absolute humidity ( $80 \text{ g/m}^3$ ) is 18 times smaller than the absolute humidity of the injected mixture ( $1,420 \text{ g/m}^3$ ) on the upstream side. This means that most of moisture is

retained by the concrete sample. This is confirmed by Haniche et al. [19] where a similar test made on High Performance Concrete (HPC) showed that all of the water vapor injected condenses in the concrete sample, causing a liquid transfer. By chemical analysis of the water extracted at the outlet of the sample, the authors also highlight the interaction between water vapor and concrete material. These results may help to explain the influence of micro-structure and especially the pore size effect on water vapor transfer through concrete. As illustrated in Fig. 8, the volume of fine pores is large enough to increase the condensation phase.



**Fig. 8** Pore size distribution of dry concrete samples (test performed at ambient temperature on a sample previously dried at 140 °C)

This study shows that no matter what conditions are imposed, the processes involved remain the same as long as the pressure gradient is different than zero. However, it is very important to note that the stabilization time of two gases mainly depends on the injection pressure ( $P_i$ ).

### 3.2 Influence of initial water content on the air and steam mixture flow through undamaged concrete

In this section, the influence of water content located in the porous network on the gas mixture flow through concrete is studied. Table 3 gives the different values of the initial degree of saturation tested. After heating phase, the degree of saturation of each sample is measured again. The results given in Table 3 show that all of the free water disappears after the heating process.

Graphs of the time evolution of the relative value of nitrogen leakage rate ( $Q_0/Q_{0,0}$ ) and the relative value of output absolute humidity ( $a_s/a_{s,TS}$ ) at different levels of initial degree of saturation are shown in Figs. 9 and 10 respectively. From these figures and the values given in Table 4, four observations can be highlighted:

- The three phases depicted in Fig. 6 for dry concrete sample can also be distinguished for non-saturated concrete samples.
- Time stabilization (TS) of the water vapor flow is slightly longer for dry concrete compared to partially saturated concrete (Fig. 11).

- The absolute humidity of the injected mixture on the upstream side ( $1,420 \text{ g/m}^3$ ) is 10-20 times as much as the downstream values (Table 4). This implies that, even after stabilization, most of the moisture conveyed by the upstream flow is retained by the concrete sample, regardless of the initial concrete saturation.
- The output absolute humidity increases with the initial degree of saturation ( $S_r$ ) of the sample (Table 4). The nitrogen leakage seems to decrease with the initial degree of saturation (except for  $S_r \leq 24\%$ ) (Fig. 9). From the output humidity value, one can assess the RH of the mixture exiting the test chamber and then the partial pressures of vapor ( $P_v$ ) and nitrogen ( $P_{N_2}$ ) in the mixture [28]. These values are given in Table 5. They allow to obtain the ratio  $r$  between the total mixture and the dry nitrogen output flows ( $\approx (P_v + P_{N_2})/P_{N_2}$ ). From dry to 85% saturated concrete, this ratio varies between 1.18 and 1.35. It confirmed that the total gas leakage through partially saturated concrete is lower than in dry concrete but the difference is less than indicated by the dry nitrogen leakage. These observations show that the initial saturation has a sizable influence, but just on the marginal residual humidity of the nitrogen exiting the test chamber.

Let us evaluate first the total water retained by the sample after the test. By equating the input and output nitrogen flow rate, Eq. (1) allows to quantify the upstream water flow  $Q_W^I$  (g/h) injected in the system [28]:

$$Q_W^I = 60 \times 10^{-3} \times Q_0 \rho_0 \frac{M_W}{M_{N_2}} \times \frac{P_v}{P_t - P_v}, \quad (1)$$

where  $Q_0$  (mL/min) is the nitrogen flow rate,  $P_t$  (Pa) is the total pressure at the upstream side,  $P_v = RH \times P_{vsat}(T)$  is the partial pressure of water vapor,  $P_{vsat}$  (Pa) the saturated vapor pressure of water at temperature  $T$  (K),  $M_W$  (g/mol) and  $M_{N_2}$  (g/mol) are the water and nitrogen molar mass and  $\rho_0$  is the nitrogen density at 0 °C and 1.013 bar.

The downstream water flow rate  $Q_W^O$  (g/h) at each stage from the beginning of a test to the final stabilization is quantified by the following equation:



**Table 3** Different values of the degree of saturation tested

Initial degree of saturation (%)	0	24	46	85
Degree of saturation after preheating phase (%)	0	1	1	3

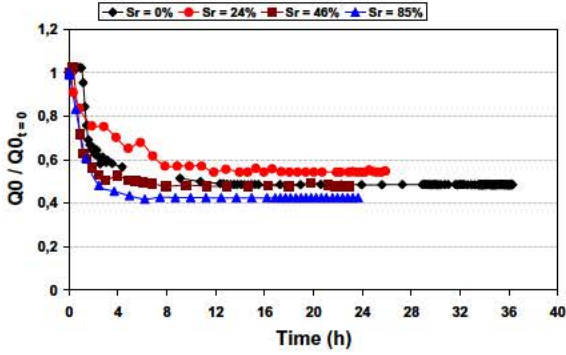


**Fig. 9** Evolution of the nitrogen leakage rate for different degrees of saturation

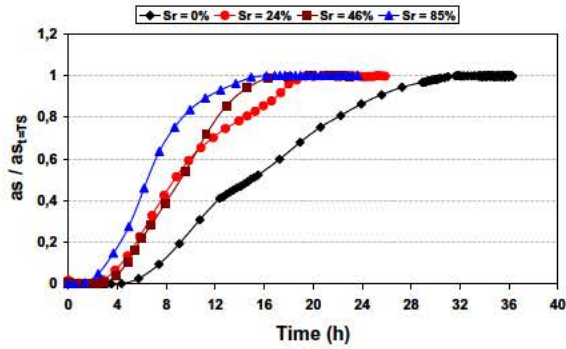


**Fig. 10** Evolution of the output absolute humidity for different degrees of saturation

**Table 4** Initial nitrogen leakage rate value ( $t = 0$  s) and output absolute humidity values at flow stabilization time for different degrees of saturation

SR (%)	0	24	46	85
Input absolute humidity (g/m <sup>3</sup> )	1,420			
Downstream measurement				
$Q_{0-t=0}$ (mLn/min)				
SP1	115.41	111.60	96.25	88.88
SP2	150.39	131.40	97.35	92.32
Mean values	133	122	97	91
$a_s/a_{s1-TS}$ (g/m <sup>3</sup> )				
SP1	85.68	101.74	107.53	123.92
SP2	71.52	90.66	105.27	148.68
Mean values	79	96	107	136

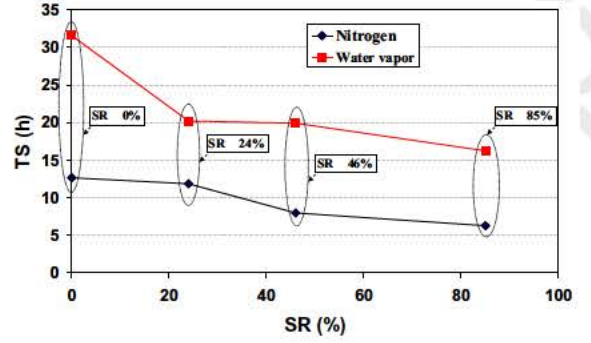


**Fig. 11** Time stabilisation (TS) vs. degree of saturation (SR)

**Table 5** Molar ratio of the mixture gas exiting the test chamber with different initial degrees of saturation

SR (%)	0	24	46	85
RH (%)	4.17	5.07	5.65	7.18
$P_v$ (bars)	0.15	0.18	0.20	0.26
$P_{N_2}$ (bars)	0.85	0.82	0.80	0.74
$r$	1.18	1.22	1.26	1.35

$$Q_W^O = 60 \times 10^3 \times Q_0 \rho_0 \frac{M_W}{M_{N_2}} \times \left( \frac{a_s RT / M_W}{P_{atm} - a_s RT / M_W} \right), \quad (2)$$

where  $a_s$  ( $\text{g}/\text{m}^3$ ) is the output absolute humidity.

By assuming that the concrete doesn't affect the injected mixture, the total water retained by the sample during the test may be assessed by integrating in time the difference between the input and output water flow rate.

Based on Table 4 and Figs. 9 and 10, an estimate gives water retention of 134, 102, 53, and 47 g for initial degrees of saturation 0, 24, 46 and 85 % respectively. It means that a significant change on the degree of saturation takes place during the moisture flow process.

Let us now consider the case of an initially dry concrete sample. Previous observations show that at a given temperature, the presence of RH in the concrete environment generates physical phenomena such as molecular adsorption (for lower RH) and capillary condensation (for higher RH) [3]. At the thermodynamic equilibrium, the amount of adsorbed water can be expressed thanks to the moisture sorption isotherm [16, 35]. At  $T = 140^\circ \text{C}$  and  $\text{RH} = 75 \%$ , the amount of adsorbed water is about 28 % of the pore volume. However this estimate is only valid from a static point of view. If the total amount of evaporable water is about 300 g ( $6 \% \times 5,000 \text{ g}$  where 5,000 g is the mass of the sample (Fig. 2), the final saturation of the dry sample should be 45 % after 36 h flushing with  $\text{RH} = 75 \%$ . This implies that dry concrete is characterized by higher moisture retention which progressively reduces the concrete permeability. Accordingly, this delays the appearance of water vapor at the output of the concrete sample (phase I is longer Fig. 10), delays gas stabilization (Figs. 9, 10), and reduces the water vapor leakage (Table 4).

In the case of an initially partially saturated concrete sample, several phenomena at the micro-structural scale take place during the heating phase. From a physical point of view, among the most important ones, there is capillary water evaporation from the porous network (after heating phase, the saturation of the samples tends to zero Table 3), the adsorbed water release and the cement hydrates dehydration [11]. These phenomena, mainly capillary effects, are associated with hydrostatic stresses generating damages that can alter the pore structure. For oven-dried concrete, Gallé [10] shows that the stresses related to the surface tension of the receding water menisci generate a collapse of some of the fine pores and consequently an increase in the volume of larger pores. Accordingly, when the gas mixture is injected,

the adsorption phenomenon (which occurs in fine pores) is not very significant and the water vapor flows more easily (Fig. 10) with a relatively shorter stabilization time (Fig. 11).

From Table 4, after stabilization, the estimate of the water retained shows that the final saturation should be 35, 20 and 18 % for 24, 46, and 85 % saturated concretes respectively. Thus, at increasing initial saturation levels, the moisture retention process is progressively reduced and the output absolute humidity increases. Another "thermo-hydro-mechanical" factor contributes to the increase in output absolute humidity. Indeed, as the gas overpressures are assumed to be completely dissipated at the end of the pre-heating phase [25, 30] the higher value of water vapor leakage rate could be explained by the material cracking and thermo-chemical degradation. As suggested by Noumowé et al. [33], by heating moist concrete above the boiling point, the endothermic nature of the free water vaporization and the water thermal expansion create locally high thermal gradients and high vapor pressure in the concrete. Accordingly, this high pore pressure generates either an expansion of pores by breaking down some partition walls or serves to trigger micro-cracks. Consequently, the pore volume available for water and gas increases significantly. Moreover, the level of tensile stresses induced by the thermal expansion of the water, from which results micro-cracks opening, depends on the amount of the free water content. Finally, higher initial moisture contents implies anyway a lower degree of saturation after stabilization, a higher porosity, and then a higher vapor content in the leaking gas.

The nitrogen leakage rate (Fig. 9 and Table 4) seems to decrease when the degree of saturation increases. It is obvious that this cannot be due to the free water inside the macropores because all of it is supposed to be vaporized. Similarly, the amount of condensed vapor (which tends to create a plug effect) is sufficiently less to be the origin of such behavior (as specified before, the adsorption/condensation phenomenon observed during the first hours following the injection is less important in partially concrete than in dry concrete). However, as written below, since the moisture is supposed to be transported both in vapor and water phases [2, 19], it can be assumed that when the equilibrium is reached, the increase of output absolute humidity with the initial degree of saturation leads to the decrease of the pore volume available for

nitrogen flow. Therefore, the nitrogen leakage rate also decreases.

### 3.3 Influence of mechanical loading on air steam flow through partially saturated concrete

In this section, the effect of compressive loading on air and water vapor leakage rate is studied. In order to couple the damage effect to that of the degree of saturation, several tests were performed on partially saturated concrete samples under different levels of compressive loading. The experimental conditions are the same as those given in Table 2. Figure 12 shows the evolution of the relative value of the nitrogen leakage rate (nitrogen leakage rate under loading/nitrogen leakage rate with loading equal to 5 kN) as function of the applied stress level for all sample tested. The evolution of the nitrogen leakage rate ( $Q_0$ ) can be divided into two main phases for all the studied saturation degrees. During the first phase,  $Q_0$  decreases slightly and then it increases until reaching its initial value. The second phase is characterized by a significant increase of  $Q_0$ . The transition between phases 1 and 2 occurs at a stress level of about 70–80 % of the ultimate compressive strength. These observations are similar to results obtained for nitrogen permeability tests on dry concrete samples [6, 21]. Apart from the initial degree of saturation level, Fig. 13 also highlights two main phases of evolution of the output absolute humidity ( $a_s$ ). Beyond 70–80 % of  $f_c$ , it begins to increase rapidly while it stays almost constant below this threshold value.

For both curves (Figs. 12, 13), the first phase is attributed to the contraction of the solid structure

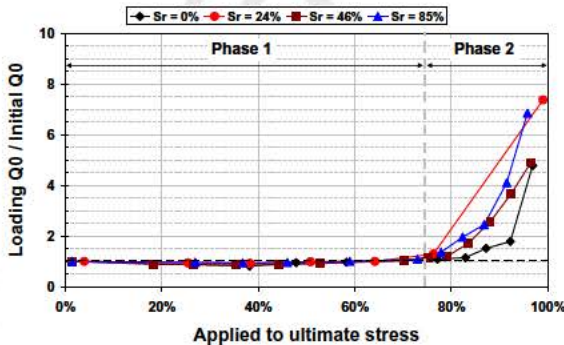


Fig. 12 Evolution of the leakage rate of dry air for partially saturated concrete samples under an increasing loading

under loading [5, 6]. This compaction behavior of the concrete sample leads to the partial closure of the intrinsic pores and micro-cracks. On the other side, the effect of initial water content on air and steam mixture flow through loading concrete samples seems to be absent. However, the nitrogen permeability test performed in our previous research [28], it was shown that before 70–80 % of  $f_c$ , there is a competitive action between mechanical loading and initial water content on gas permeability. Thus, absence of the effect of concrete water content on the air and steam leakage rates could be explained by the fact that the water remaining after the drying is not sufficiently important.

The increase in both parameters ( $Q_0$  and  $a_s$ ) during the second phase is attributed to the diffuse micro-cracking which is characterized by low level damage (from 0 to 0.15). Indeed, a uni-axial compressive load beyond 70–80 % of the ultimate strength induced micro-cracking increasing and so causing an increase of the permeability of concrete [6, 21, 29]. It is difficult to see the influence of the initial water content on the hydraulic behavior of damaged concrete. The results show that the increase in gas mixture leakage rate is independent of the sample moisture content but it is more sensitive to the development and coalescence of cracks. Further studies on partially saturated concrete with localized cracks opening evaluation are needed to better explain these results.

Finally, Figs. 12 and 13 show that under mechanical loading, there is a link between the closing of pores and cracks on one hand, and the creation and growth of cracks on the other hand. In this relationship

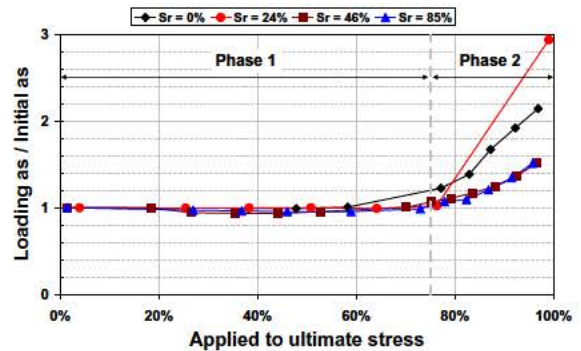


Fig. 13 Evolution of the output absolute humidity for partially saturated concrete samples under an increasing loading as a function of mechanical loading

there are two phases. During the first phase, the mean volumetric behavior of the concrete is strictly contracting, and then the gas mixture leakage rate decreases slightly. In contrast, the second phase is characterized by micro-cracking generation, causing significantly increase of gas mixture leakage rate.

#### 4 Conclusions

The results reported in this study can be summarized as follows:

- (1) For both fluids (air and steam), the stabilization state is reached after several hours of permeability test. This stabilization time decreases when the degree of saturation increases. The free water which induces a large pore-crack network during the heating phase is mainly responsible of this behavior. Thus, the amount of fine pores is reduced. Consequently the adsorption/condensation phenomena observed in dry concrete during the first hours following injection are less important in partially saturated concrete and the gases flow more easily.
- (2) The degree of saturation level significantly affects the gas mixture leakage rate through undamaged concrete samples. The results suggest that in an isothermal system (with temperature above the dew point temperature of water), the more free water the concrete contains, the higher is the leak rate of steam. This is due to the capillary effect generated by the vaporization of free water and the thermal expansion of water, which lead to create strong moisture gradients able to cause micro-crack and so to increase the available volume network. Moreover, it is assumed that the greater the initial water content, the more concrete porosity increases, and thus greater will be the water vapor leakage rate. Nevertheless, as the water vapor flow increases, the pore network available for nitrogen seems to decrease inducing the decrease of the nitrogen flow rate.
- (3) Two main phases characterize the evolution of the gas mixture leakage rate when a compressive stress is applied on the concrete sample. Firstly, when the applied stress level is below 70 % of the ultimate strength, the output

absolute humidity and the nitrogen leakage rate stay almost constant or decrease and then increase slightly. Secondly when the concrete sample is damaged (applied stress exceeds 70-80 % of the ultimate strength), the leakage rate of both gases significantly increases. During the mechanical loading, the influence of initial water content appears to be negligible and becomes insignificant when the material is damaged.

In this experimental study, we try to highlight the influence of the water content on the air and steam mixture flow through concrete samples. In the future, it could be of interest to analyze the influence of the water content distribution, thermal gradient and their effect on the measurements of crack openings and flow rates.

**Acknowledgments** This study has been performed in the Project ECOBA coordinated by Prof. A. LOUKILI and funded by the French National Research Agency (ANR Agence Nationale de la Recherche) under Grant Number ANR 09 BLAN 0406. ANR and the partners of project are gratefully acknowledged.

#### References

1. Abbas A, Carcasses M, Olivier J P (1999) Gas permeability of concrete in relation to its degree of saturation. *Mater Struct* 32:3-8
2. Anderberg Y (1997) Spalling phenomena of HPC and OC. In: *Proceedings of international workshop on fire performance of high strength concrete*. Nation Institute of Standards and Technology, Gaithersburg, pp 69-73
3. Baroghel Bouny V (2007) Water vapour sorption experiments on hardened cementitious materials Part I: essential tool for analysis of hygral behavior and its relation to pore structure. *Cem Concr Res* 37:414-437
4. Billard Y, Debicki G, Coudert L (2005) Leakage rate through a non cracked concrete wall, comparison between two situations: air pressure test and accident conditions. *Nucl Eng Des* 235:2109-2123
5. Cerny R, Madera J, Podebradska J, Toman J, Drchalova J, Klecka T, Jurek K, Rovnanikova P (2000) The effect of compressive stress on thermal and hygric properties of Portland cement mortar in wide temperature and moisture ranges. *Cem Concr Res* 30:1267-1276
6. Choinska M, Khelidj A, Chatzigeorgiou G, Pijaudier Cabot G (2007) Effects and interactions of temperature and stress level related damage on permeability of concrete. *Cem Concr Res* 37:79-88
7. Daian J F (1988) Condensation and Isothermal water transfer in cement mortar: part I pore size distribution, equilibrium water condensation and imbibition. *Transp Porous Media* 3:563-589

8. Daian J F (1989) Condensation and isothermal water transfer in cement mortar: part II transient condensation of water vapor. *Transp Porous Media* 4:1 16
9. Dal Pont S, Durand S, Schrefler BA (2007) A multiphase thermo hydro mechanical model for concrete at high temperatures finite element implementation and validation under LOCA load. *Nucl Eng Des* 237:2137 2150
10. Gallé C (2001) Effect of drying on cement based materials pore structure as identified by mercury intrusion porosimetry: a comparative study between oven , vacuum , and freeze drying. *Cem Concr Res* 31:1467 1477
11. Gallé C, Sercombe J (2001) Permeability and pore structure evolution of silicocalcareous and hematite high strength concretes submitted to high temperatures. *Mater Struct* 34:619 628
12. Gawin D, Majorana CE, Schrefler BA (1999) Numerical analysis of hygrothermal behaviour and damage of concrete at high temperature. *Mechan Cohes Frict Mater* 4:37 74
13. Gawin D, Schrefler BA, Pesavento F (2002) Modelling of hydro thermal behaviour and damage of concrete at temperature above the critical point of water. *Int J Numer Anal Methods Geomech* 26:537 562
14. Gawin D, Alonso C, Andrade C, Majorana CE, Pesavento F (2005) Effect of damage on permeability and hygro thermal behaviour of HPCs at elevated temperatures : part 1. Experimental results. *Comput Concr* 2:189 202
15. Gawin D, Pesavento F, Schrefler BA (2006) Towards prediction of the thermal spalling risk through a multi phase porous media model of concrete. *Comput Methods Appl Mech Eng* 195:5707 5729
16. Gawin D, Pesavento F, Schrefler BA (2011) What physical phenomena can be neglected when modelling concrete at high temperature? A comparative study. Part 1: physical phenomena and mathematical model. *Int J Solids Struct* 48:1927 1944
17. Granger L, Fleury F, Touret J P (2001) Mechanical and leaktightness predictions for nuclear power plant containments in accidental conditions. *Nucl Eng Des* 203:39 55
18. Greiner U, Ramm W (1995) Air leakage characteristics in cracked concrete. *Nucl Eng Des* 156:167 172
19. Haniche R, Debicki G, Bouamrane A, Zeltz E (2011) Gas transfers and flow process through concrete maintained in temperature. In: 2nd International RILEM workshop on concrete spalling due to fire exposure, pp 95 102
20. Herrmann N, Niklasch C, Stegemann M, Stempniewski L (2002) Investigation of leakage behaviour of reinforced concrete walls. *Structures and Buildings Materials. Institute of Reinforced Concrete, University of Karlsruhe, Karlsruhe*
21. Hoseini M, Bindiganavile V, Banthia N (2009) The effect of mechanical stress on permeability of concrete: a review. *Cem Concr Compos* 31:213 220
22. Jacobs F (1998) Permeability to gas of partially saturated concrete. *Mag Concr Res* 50:115 121
23. Janotka I, Bagel L (2002) Pore structures, Permeabilities, and Compressive strengths of concrete at temperatures up to 800°C. *ACI Mater* 99:196 200
24. Jooss M, Reinhardt H W (2002) Permeability and diffusivity of concrete as function of temperature. *Cem Concr Res* 32:1497 1504
25. Kalifa P, Menneteau F D, Quenard D (2000) Spalling and pore pressure in HPC at high temperatures. *Cem Concr Res* 30:1915 1927
26. Kameche ZA, Ghomari F, Choinska M, Khelidj A (2014) Assessment of liquid water and gas permeability of partially saturated ordinary concrete. *Cem Concr Res* 65:551 565
27. Lewis RW, Schrefler BA (1998) The finite element method in the static and dynamic deformation and consolidation of porous media. Wiley, Hoboken
28. Medjigbodo S, Darquennes A, Aubernon C, Khelidj A, Loukili A (2013) Effects of the air steam mixture on the permeability of damaged concrete. *Cem Concr Res* 54: 98 105
29. Meziani H, Skoczylas F (1999) An experimental study of the mechanical behaviour of a mortar and of its permeability under deviatoric loading. *Mater Struct* 32:403 409
30. Mindeguia J C, Pimienta P, Noumowé A, Kanema M (2010) Temperature, pore pressure and mass variation of concrete subjected to high temperature experimental and numerical discussion on spalling risk. *Cem Concr Res* 40:477 487
31. Monlouis Bonnaire JP, Verdier J, Perrin B (2004) Prediction of the relative permeability to gas flow of cement based materials. *Cem Concr Res* 34:737 744
32. Niklasch C, Coudert L, Heinfing G, Hervouet C, Masson B, Herrmann N, Stempniewski L (2005) Numerical investigation of the leakage behavior of reinforced concrete walls. In: The 11th International topical meeting on nuclear thermal hydraulics (NURETH 11), France, October 2 6
33. Noumowé A, Clastres P, Debicki G, Costaz J L (1996) Transient heating effect on high strength concrete. *Nucl Eng Des* 166:99 108
34. Noumowé A, Siddique R, Debicki G (2009) Permeability of high performance concrete subjected to elevated temperature (600 °C). *Constr Build Mater* 23:1855 1861
35. Pesavento F (2000) Non linear modeling of concrete as multiphase material in high temperature conditions. PhD thesis, Università degli Studi di Padova
36. Picandet V, Khelidj A, Bastian G (2001) Effect of axial compressive damage on gas permeability of ordinary and high performance concrete. *Cem Concr Res* 31:1525 1532
37. Picandet V, Khelidj A, Bellegou H (2009) Crack effects on gas and water permeability of concretes. *Cem Concr Res* 39:537 547
38. Quenard D, Carcasses M (1999) Gas permeability of concrete: definition of a preconditioning procedure for measurements and crossover trials. *Durab Build Mater Compon* 8 1:236
39. Shekarchi M, Debicki G, Granger L, Billard Y (2002) Study of leaktightness integrity of containment wall without liner in high performance concrete under accidental conditions I. Experimentation. *Nucl Eng Des* 213:1 9
40. Simon H, Nahas G, Coulon N (2007) Air steam leakage through cracks in concrete walls. *Nucl Eng Des* 237: 1786 1794
41. Sugiyama T, Bremner TW, Holm TA (1996) Effect of stress on gas permeability in concrete. *ACI Mater J* 93:443 450
42. Suzuki T, Takiguchi K, Hotta H (1992) Leakage of gas through concrete cracks. *Nucl Eng Des* 133:121 130

43. Villain G, Baroghel Bouny V, Kounkou C, Hua C (2001) Measuring the gas permeability as a function of saturation rate of concrete. Fr J Civ Eng 5:251-268 [Transfer in concrete and durability, In French]

44. Zeiml M, Lackner R, Leithner D, Eberhardsteiner J (2008) Identification of residual gas transport properties of concrete subjected to high temperatures. Cem Concr Res 38:699-716

Accepted Manuscript